RSC Advances

PAPER

View Article Online
View Journal | View Issue

Cite this: *RSC Adv.*, 2015, **5**, 32350

Melt free radical grafting of glycidyl methacrylate (GMA) onto fully biodegradable poly(lactic) acid films: effect of cellulose nanocrystals and a masterbatch process

Weijun Yang, Franco Dominici, Elena Fortunati, José M. Kenny and Debora Puglia*

Received 15th January 2015
Accepted 27th March 2015

DOI: 10.1039/c5ra00894h

www.rsc.org/advances

This article reports the preparation, by means of a masterbatch procedure, of poly (lactic acid) (PLA)/cellulose nanocrystal (CNC) films *via* premixing 1% wt of CNC into PLA or glycidyl methacrylate (GMA) grafted PLA (g-PLA). These films were obtained by reactive extrusion and subsequent film processing. In this study, 10% wt of GMA with respect to neat PLA was used in the extrusion phase, after that a final grafting degree of 5.69% was obtained. The film obtained by using the masterbatch steps were compared with the system obtained by a direct extrusion of 1% wt of CNC in PLA/g-PLA. Thermogravimetric, crystallization and mechanical properties, as well as morphology of CNC reinforced PLA nanocomposites were characterized. Differential scanning calorimetry and thermogravimetric analysis showed enhanced crystallization ability and an improved heat resistance for the resulting nanocomposites obtained after the use of masterbatches, for example field emission scanning electron microscopy confirmed that the masterbatch preparation procedure was beneficial to the dispersion of CNC in the final nanocomposites. Furthermore, different mechanical performance was obtained when using different masterbatches, which were considered to contribute to extend the applications of PLA based composites as food packaging materials in different sectors.

Introduction

Research on biodegradable polymer nanocomposites has attracted both considerable industrial and academic attention in recent years, due to their being environmentally friendly, having good performance, design flexibility, lower life-cycle costs and a large applicability range in various industrial fields. Both the nanofillers and matrix come from bio-based, renewable agricultural resources, making them competitive with petroleum-derived materials.[1–4] In the food packaging industry, there is a trend that renewable plastics will substitute petroleum based plastics with lower environmental impact, among which poly(lactic acid) (PLA) is a very promising material because of its excellent mechanical properties, transparency and commercial availability. Nonetheless, some properties, such as gas and water vapour permeability and thermal stability, are somewhat poor for some specific applications. In this context, the addition of nanoparticles as polymer additives contributes to enhance the barrier to gases due to the synergistic tortuosity, crystal nucleation and chain immobilization effects.[1–5]

Cellulose is one of most abundant carbohydrate polymers produced by biomass, from which high modulus nanocrystals (CNC) can be extracted. These nanosized particles have been recognized as important bio-based fillers to enhance the biopolymer performance, in terms of mechanical, thermal and barrier properties. In the meanwhile, they present the advantage of being renewable when compared to other inorganic fillers, which have been widely proposed to reinforce PLA and develop biodegradable materials.[1,6–9] However, homogeneous dispersion of cellulose nanoparticles is difficult to be achieved by means of traditional melt processing techniques, due to the high tendency of CNC to form agglomerates as a consequence of the presence of hydroxyl groups on the particle surfaces and their high specific surface area.[10,11] In order to promote the compatibility between the components, functionalization of cellulose nanostructures and PLA can be also carried out (in solution as well as in the melt) using either surface silanization, grafting of reactive groups or polymer chains.[12,13] Li *et al.*[14] prepared a novel copolymer of PLA and glycidyl methacrylate (PLA-*co*-PGMA) by free radical polymerization and used it to modify the cellulose surface. Interfacial thermodynamic properties were studied and the results suggested that PLA-*co*-PGMA was efficient in the modification of bacterial cellulose (BC) nanofibril surface and in improvement of compatibility of PLA-cellulose composites. Fortunati *et al.*[15] also studied the blend of

University of Perugia, Civil and Environmental Engineering Department, UdR INSTM, Strada di Pentima 4, 05100 Terni, Italy. E-mail: debora.puglia@unipg.it; Fax: +39 0744492950; Tel: +39 0744492916

PLA with an ethylene-vinyl acetate–GMA copolymer (EVA–GMA), and their composites with cellulose microfibers (CF); the results showed that the presence of EVA–GMA contributed to improve the interfacial adhesion between cellulose fibres and PLA, due to interactions of the epoxy groups of GMA with hydroxyls of CF. By using the Fourier Transform Infrared Spectroscopy (FTIR), X-ray photoelectron spectroscopy (XPS) and transmission electron microscopy (TEM), Stenstad *et al.*[16] confirmed that the epoxy functionality was introduced onto the microfibrillated cellulose (MFC) surface by oxidation with cerium(IV) followed by grafting of GMA and the length of the polymer chains could be varied by regulating the amount of GMA added. In a study by Martínez-Sanz *et al.*,[17] poly(glycidyl methacrylate) (PGMA) was grafted onto bacterial cellulose nanowhiskers (BCNW) by means of a redox-initiated free radical copolymerization reaction. The neat and the PGMA-grafted BCNW were subsequently incorporated as fillers into the PLA matrix. PGMA grafting improved both matrix-filler adhesion and the dispersion of cellulose nanocrystals. The incorporation of both neat and PGMA-grafted BCNW significantly reduced the oxygen permeability of PLA. Furthermore, increased elastic modulus and tensile strength were observed for all the nanocomposites, especially when the concentration of nanocrystals was around the percolation threshold, *i.e.* 3% wt, but only nanocomposites containing PGMA-grafted BCNW preserved the ductility of neat PLA. Pracella *et al.*[18] functionalized PLA and CNC by radical grafting of glycidyl methacrylate (GMA) and pre-dispersed CNC in poly(vinyl acetate) (PVAc) emulsion; their results showed that functionalized components (PLA–GMA, CNC–GMA) and/or PVAc dispersed CNC both improved the phase distribution of nanofiller and tensile properties, compared to the binary PLA/CNC nanocomposites. Most above listed researches focused on the effects of dosage and modification of nanofillers or PLA matrix on the properties of resulted nanocomposites. Jonoobi *et al.*,[7] in order to improve the nanofiber dispersion, prepared a masterbatch of PLA/cellulose nanofibers (CNF) by solvent casting before extrusion. The morphology studies of PLA and its nanocomposites showed that a relatively good dispersion was achieved as no CNF aggregates were visible in the fracture surfaces of the PLA nanocomposites with 1 and 3% wt of CNF, hence an enhancement of the mechanical performances of the final materials was obtained. Arrieta *et al.*[19] blended a PLA–poly(hydroxybutyrate) (PHB) masterbatch system, which was granulated into pellets and then melted in the microextruder (1 min) while 5% wt of CNC or surfactant-modified CNC (s-CNC) were subsequently added and mixed, and the results revealed that the use of a masterbatch improved the dispersion of CNC and s-CNC in the final nanocomposite films and made easier the processability between PLA and PHB.

In this study, we highlight the preparation of different masterbatches by premixing the 1% wt of CNC into PLA or modified PLA matrix and finally processed into films. Thermal and mechanical properties were tested and reported here, with the aim to evaluate their suitability for the food packaging sector, expecting to optimize the approaches to process the nanocomposites and to provide some reference for industrial manufacture and practical application of CNC reinforced bioplastic nanocomposites.

Experimental

Materials

Poly(lactic acid) (PLA 3251D), with a specific gravity of 1.24 g cm^{-3}, a relative viscosity of *ca.* 2.5, and a melt flow index (MFI) of 35 g/10 min (190 °C, 2.16 kg) was supplied by Nature Works LLC, USA. Glycidyl methacrylate (GMA 779342), with a density of 1.042 g mL^{-1} at 25 °C, and dicumyl peroxide (DCP 329541), with a density of 1.56 g mL^{-1} at 25 °C, were supplied by Sigma-Aldrich. PLA pellets were dried in an oven at 40 °C for overnight. Microcrystalline cellulose (MCC, dimensions of 10–15 μm) was supplied by Sigma-Aldrich.

Methods

Cellulose nanocrystal (CNC) synthesis. CNC suspension was prepared from MCC by sulphuric acid hydrolysis following the recipe used by Cranston.[20,21] Generally, hydrolysis was carried out with 64% (wt/wt) sulphuric acid at 45 °C for 30 min with vigorous stirring, followed by diluting the suspension into a 20-fold deionised water to quench the reaction. The suspension was then centrifuged at 4500 rpm for 20 min to concentrate the cellulose and to remove excess aqueous acid. The resultant precipitate was dialyzed against water for 5 days to further eliminate the acid until a pH of *ca.* 7.0 was obtained. Mixed bed ion exchange resin (Dowex Marathon MR-3 hydrogen and hydroxide form) was added to the cellulose suspension for 24 h and then removed by filtration, which ensured that all ionic materials were removed except the H^+ counter ions associated with the sulphate groups on the CNC surfaces. An ultrasonic treatment by means of a tip sonicator (Vibracell, 750) for 5 min was then performed. The pH of cellulose nanocrystal suspensions was raised to approximately 9 by the addition of 1.0% (wt/wt) (0.25 mol L^{-1}) NaOH in order to stabilize the cellulose. The resultant cellulose nanocrystal aqueous suspension was approximately 0.5% (wt/wt) by weight and the yield was *ca.* 20%. The solid CNC was collected by freeze-vacuum dry method (lyophilizer Virtis B.T. 2K ES).

Preparation of masterbatches (MBs). In order to determine the effects of processing procedures on the properties of the PLA based nanocomposites, in this study we fixed the content of CNC and PLA grafted with GMA (g-PLA) to 1% wt and 15% wt, respectively, in the resulted nanocomposites. The compositions of different masterbatches are shown in Table 1.

Table 1 Masterbatches for preparation of PLA nanocomposites

MBs	Composition	Dwell time (min)
MB1	g-PLA	8
MB2	PLA + 1.17% CNC	6 + 2
MB3	g-PLA + 6.67% CNC	6 + 2
MB4	Neat PLA	8

Grafting of GMA onto the PLA (MB1 and MB3) was performed in a twin-screw microextruder (DSM Explorer 5&15 CC Micro Compounder) in the presence of DCP as initiator. The DCP and GMA (DCP/GMA = 1/10 in weight) were mixed and the solution was sprayed onto the dried PLA matrix. The GMA content was fixed at 10% wt of the PLA weight. The mixture of GMA, PLA and initiator DCP was introduced into the microextruder. Screw speed of 100 rpm and mixing time of 8 min were used in order to realize the grafting reaction, while a temperature profile of 165–175–180 °C was chosen.

The different masterbatches were obtained by mixing various amounts of CNC with PLA or g-PLA. In details, the following processing conditions were applied:

- MB1 consisted of grafted PLA (g-PLA) prepared in the conditions above reported (total time of reaction in the extruder of $t = 8$ minutes);

- MB2 was obtained through incorporation of 1.17% wt of CNC into PLA matrix, with incorporation of CNC (mixing time 2 minutes) after 6 minutes of PLA heating, in order to prevent the thermal degradation for CNC;

- MB3 was obtained through incorporation of 6.67% wt of CNC into g-PLA matrix, with incorporation of CNC (mixing time 2 minutes) after 6 minutes of g-PLA heating;

- MB4 consisted of neat PLA, produced under the same parameters as described in the cases of MB1, MB2 and MB3 (total time of mixing = 8 minutes).

PLA nanocomposite processing. PLA and PLA nanocomposite films were manufactured by using a twin-screw microextruder as well. Conditions of 100 rpm screw speed, 2 min of dwell time and a kneading temperature of 180–195–210 °C were employed to optimize material final properties, after which, a film forming process with a head force of 180 N and a die temperature of 200 °C was performed, in order to obtain PLA and PLA nanocomposite films with a thickness ranged from 20 up to 80 μm. The materials designed as neat PLA and g-PLA were regarded as controls, while the PLA nanocomposite films having the codes PLA/1CNC and g-PLA/1CNC consisted of 99% wt MB4 and MB1, respectively, and 1% wt of CNC. The system containing 15% wt of MB1 and 85% wt of MB2 was denoted as g-PLA/PLA-1CNC, while g-PLA-1CNC/PLA represented the material composed of 16% wt of MB3 and 84% wt of MB4. Finally, g-PLA/PLA/1CNC was indicated as the material obtained through the reactive mixture of 15% wt MB1, 84% wt = MB4 and 1% wt CNC. Thus, the contents of CNC and g-PLA in the resulted nanocomposite films were 1% wt and 15% wt, respectively. These formulations are reported in Table 2.

Table 2 Nanocomposite formulations

Materials	MB1 (% wt)	MB2 (% wt)	MB3 (% wt)	MB4 (% wt)	CNC (% wt)	Dwell time (min)
PLA				100		2
g-PLA	100					2
PLA/1CNC				99	1	2
g-PLA/1CNC	99				1	2
g-PLA/PLA-1CNC	15	85				2
g-PLA-1CNC/PLA			16	84		2
g-PLA/PLA/1CNC	15			84	1	2

Characterizations

Fourier transform infrared spectrometry (FTIR) analysis. FTIR analysis was performed by means of a Jasco FTIR 615 spectrometer instrument (Japan). The samples were scanned in the frequency range 500–4000 cm^{-1} operating in ATR (attenuated total reflectance) mode. In case of PLA and PLA-g-GMA, FTIR analysis was performed on thin films prepared by solvent casting from a chloroform (supplied by Sigma-Aldrich) solution after removal of residual GMA and homopolymer.[22]

Determination of the GMA content. Purification of g-PLA was performed drying g-PLA and neat PLA (1.50 ± 0.01 g) and dissolving them in 40 mL of chloroform. The solution was vigorously stirred for 45 min in a hot plate stirrer (Thermolyne Mirak hot plate/stirrer; Sigma-Aldrich Corp., Saint Louis, MO). Finally, the suspension was precipitated with a large excess of ethanol. The products were washed several times with ethanol to remove the residual GMA and homopolymer, and then dried to a constant weight in a vacuum oven at 60 °C for 24 h. The weight percentage of grafting was determined by back-titration, the most common procedure used in epoxide analysis. The grafted polymer (0.50 ± 0.02 g) was refluxed with *o*-xylene for 0.5 h, and then 5.0 ml HCl–isopropanol (0.1 mol L^{-1}) solution was added. The solution was allowed to complete the reaction for 0.5 h. The GMA content of grafted polymer was determined by titration of the residual hydrochloric acid by back-titration with standard KOH–ethanol (0.1 mol L^{-1}), and 2–3 drops of the phenolphthalein–ethanol (10 g L^{-1}) was added as an indicator. The end point was determined by colour change. The neat PLA was used as control. The grafted GMA (%) were calculated according to the following expression:

$$\text{Grafted GMA (\%)} = V_{HCl} \times N_{HCl} \times 142.2 \times 0.1/m \quad (1)$$

where V_{HCl} and N_{HCl}, were volume (mL) and normality of the standardized HCl, respectively; 142.2 was the molecule weight of GMA; m was the weight of the sample in g. In this study, 10% of the GMA (MB1) was used and the final grafting degree was 5.69%, the result was in accordance with some other researches.[14,22]

Morphology. The cellulose nanocrystal morphology was investigated by means of field emission scanning electron microscope (FESEM, Supra 25-Zeiss). Few drops of the suspension were cast onto silicon substrate, vacuum dried for 2 h and gold sputtered before the analysis. Microstructure of the PLA nanocomposite films were also investigated by FESEM, by checking the cross-section morphology of samples fractured in liquid nitrogen and followed by gold sputtering.

Differential scanning calorimeter (DSC). DSC (TA Instrument, Q200) measurements were performed in the temperature range from −25 to 210 °C at 10 °C min^{-1} under nitrogen flow; PLA and PLA nanocomposite samples (6–7 mg) were heated from −25 to 210 °C at a rate of 10 °C min^{-1} and held at 210 °C for 2 min to erase the thermal history (1st scan), then they were

cooled to −25 at 10 °C min^{-1} and reheated under the same conditions (2nd scan). Glass transition, cold crystallization and melting temperatures, indicated as T_g, T_{cc} and T_m, respectively, were determined from the first and second heating scans. The crystallinity degree (χ) was calculated from the second scan as:

$$x = \frac{\Delta H_m}{\Delta H_{m0}(1 - m_f)} \quad (2)$$

where ΔH_m is enthalpy of melting for a 100% crystalline PLA sample, taken as 93 J g^{-1} (ref. 23) and ($1 - m_f$) is the weight fraction of PLA in the sample.

Thermogravimetric analysis (TGA). TGA was carried out using a Thermo gravimetric Analyzer (TGA, Seiko Exstar 6300). The samples, approximately 8 mg, were heated from 30 to 900 °C at a heating rate of 10 °C min^{-1} under nitrogen atmosphere. The weight-loss rate was obtained from derivative thermogravimetric (DTG) data. The onset degradation temperature (T_{onset}) was defined as the 1% weight loss drawn from the TG curves after 200 °C at which the samples begin to degrade. Maximum thermal degradation temperature (T_{max}) was also collected from DTG peaks maxima, along with the residual weight percent at 600 °C.

Mechanical behavior. The mechanical performance of neat PLA and PLA nanocomposite systems was evaluated by means of tensile tests, performed on rectangular probes (100 mm × 10 mm) on the basis of UNI ISO 527 standard with a crosshead speed of 5 mm min^{-1}, a load cell of 500 N and an initial gauge length of 25 mm. Average tensile strength (σ), elastic modulus (E) and elongation at break (ε_b) were calculated from the resulting stress–strain curves. The measurements were done at room temperature and at least five samples were tested.

Results and discussion

FTIR analysis

The g-PLA (grafted polymer) was successfully prepared *via* free-radical polymerization, in which the peroxide initiator abstracted a tertiary hydrogen from the PLA chain to form a macromolecular radical, as shown in Fig. 1a, and the mechanism was revealed in a study by Xu,[24] in which *tert*-butyl perbenzoate (TBPB) was used as initiator. The FTIR spectra of neat PLA, PLA/GMA, and g-PLA are given in Fig. 1b, in which PLA/GMA indicates g-PLA without further purification after the polymerization, with unreacted residual GMA inside.

Compared with the spectrum of neat PLA, some new peaks appeared at 815, 910 and 1637 cm^{-1} in the spectrum of PLA/GMA and were associated with the carbon double bonds (815 and 1637 cm^{-1})[24] and the asymmetric stretching of the epoxy group (910 cm^{-1}).[14,18] After eliminating the unreacted GMA, the peak of epoxy group was still present, while the C=C bond was not observed in the case of g-PLA, which means that the C=C bonds disappeared after polymerization and GMA was successfully grafted onto the PLA chain. Similar results were also reported.[18]

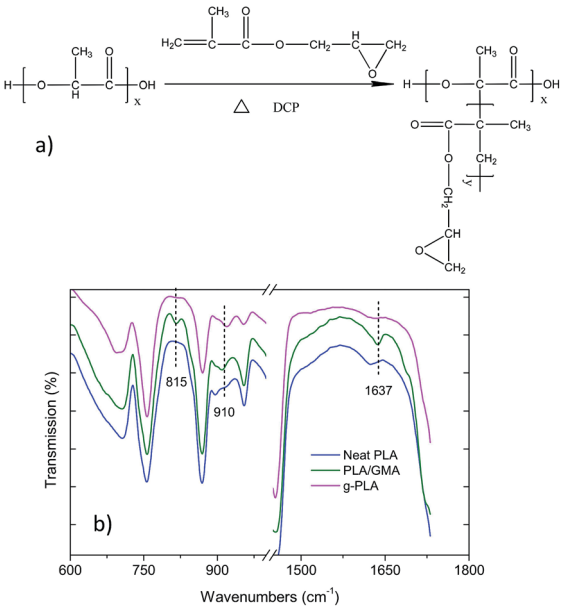

Fig. 1 (a) Mechanism of the grafting of GMA onto the PLA chain and (b) FTIR spectra of neat PLA, PLA/GMA, and g-PLA.

DSC analysis

Differential scanning calorimetry was used to investigate the glass transition (T_g), cold crystallization (T_{cc}), melting (T_m) and crystallinity (X_c) of PLA and PLA nanocomposites. Photos reported in Fig. 2a show the visual appearance of neat PLA and PLA nanocomposite films prepared with the different masterbatches, confirming that all the films have good transparency, with no effects related to the process used for the preparation of the different formulations. Fig. 2(b–d) and Tables 3 and 4

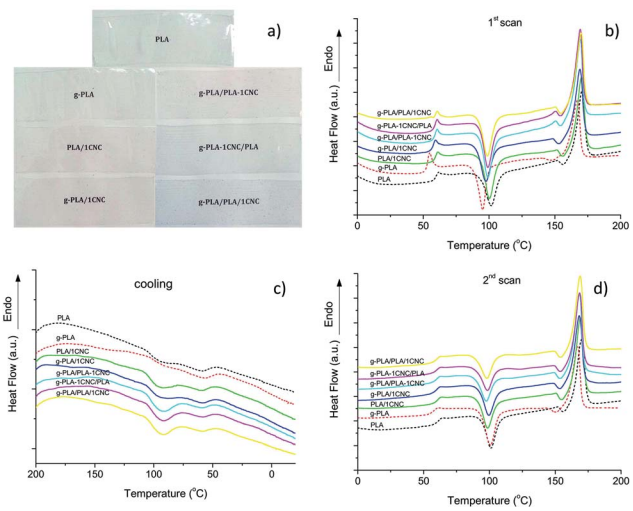

Fig. 2 Visual appearance of films (a), DSC thermograms related to the (b) first heating scan, (c) cooling scan and (d) second heating scan of neat PLA, g-PLA and PLA nanocomposite systems obtained by different masterbatch procedures.

Table 3 Thermal parameters (T_g, T_{cc} and T_m) of PLA and PLA nanocomposites derived from the first heating DSC scan of nanocomposite formulations

Materials	T_g (°C)	T_{cc} (°C)	T_m (°C)
PLA	61.3 ± 0.4	101.8 ± 0.1	170.3 ± 0.2
g-PLA	54.4 ± 0.3	94.7 ± 0.3	166.9 ± 0.3
PLA/1CNC	60.9 ± 0.1	100.2 ± 0.1	170.0 ± 0.1
g-PLA/1CNC	59.4 ± 0.3	97.7 ± 0.5	168.8 ± 0.2
g-PLA/PLA-1CNC	60.6 ± 0.3	98.7 ± 0.3	169.1 ± 0.2
g-PLA-1CNC/PLA	61.0 ± 0.1	94.2 ± 0.1	169.1 ± 0.1
g-PLA/PLA/1CNC	60.5 ± 0.1	98.2 ± 0.4	169.5 ± 0.5

Table 4 Thermal parameters (T_g, T_{cc}, T_m and χ_c) of PLA and PLA nanocomposites derived from the second heating DSC scan

Materials	T_g (°C)	T_{cc} (°C)	T_m (°C)	X_c (%)
PLA	61.5 ± 0.6	100.3 ± 0.8	169.3 ± 0.2	15.0 ± 1.0
g-PLA	57.9 ± 0.2	100.1 ± 0.4	166.5 ± 0.5	7.4 ± 3.8
PLA/1CNC	60.6 ± 0.2	98.4 ± 0.3	169.0 ± 0.2	18.8 ± 2.6
g-PLA/1CNC	60.0 ± 0.6	98.9 ± 0.4	168.2 ± 0.1	16.3 ± 1.8
g-PLA/PLA-1CNC	59.2 ± 0.6	97.1 ± 0.7	168.2 ± 0.1	24.4 ± 0.1
g-PLA-1CNC/PLA	60.4 ± 0.3	97.9 ± 0.5	168.3 ± 0.5	24.1 ± 1.4
g-PLA/PLA/1CNC	59.8 ± 0.6	97.5 ± 0.7	168.4 ± 0.3	23.2 ± 0.7

summarize the calorimetric parameters from the first and second heating scan for all materials.

To make the following discussion clearer, here we divided them into three systems, namely the first system as CNC premixed with pure PLA system (PLA, PLA/1CNC and g-PLA/PLA-1CNC), the second system as CNC premixed with g-PLA system (g-PLA, g-PLA/1CNC and g-PLA-1CNC/PLA) and the third system as the one in which CNC are introduced in the mixture without using a masterbatch procedure (g-PLA/PLA/1CNC). The low T_g, T_{cc} and T_m values detected for g-PLA at the first heating scan (Fig. 2b and Table 3) were due to the presence of high content of grafted PLA and residual GMA in the film after extrusion. In the case of PLA/1CNC and g-PLA/PLA-1CNC, a slight decrease of T_g was observed respect to PLA, and this effect can be related to the incorporation of CNC, that blocked the weak interactions between PLA chains, such as van der Waals force and hydrogen bond. An opposite tendency was indeed detected for g-PLA/1CNC and g-PLA-1CNC/PLA systems, in which CNC particles acted as claws. While in the case of neat g-PLA we observed a reduction in glass transition with respect of neat PLA (due to the plasticizing effect of GMA), in the case of systems that contains CNC, the presence of GMA contributed to improve the interfacial adhesion between CNC and PLA matrix, and this behavior can be explained considering the possible interactions of the epoxy groups of GMA with hydroxyls of CNC, that restrict the motion of PLA chain segments and increase the complex viscosity, with consequent increase of T_g.[15] Moreover, the thermogram of g-PLA, revealed a sharper endothermic peak, respect to other samples, associated to the glass transition, which it is typically attributed to a stronger stress relaxation on heating.[25] Some other studies also reported similar relaxation phenomena in plasticized PLA, confirming the presence of a compatibilizer with a plasticizing effect in the films.[1,26] It was also observed that the ability to re-crystallize increased for PLA nanocomposites, with a reduction in T_{cc} (98.7 °C of g-PLA/PLA-1CNC and 94.2 °C of g-PLA-1CNC/PLA, respectively) in comparison with neat PLA or g-PLA, since CNC served as a preferable heterogeneous nucleation agent in PLA matrix. Moreover, the grafting of GMA onto PLA matrix promoted the dispersion of CNC in matrix, representing an important factor on the different crystallization behavior of the resulted nanocomposites.[27,28]

It should be also observed that the shapes of melting peaks changed at the first heating scan. In Fig. 2b, the double melting peaks appeared on the curves of g-PLA/PLA-1CNC, g-PLA-1CNC/PLA and g-PLA/PLA/1CNC, which could be attributed to the melt/recrystallization of the α form crystal of PLA.[29] With the CNC premixing with PLA (MB2) and g-PLA (MB3), the melting peak at lower temperature becomes visible and the melting peak at higher temperature still retains. A small exothermic peak appeared prior to the major melting peak when the CNC were incorporated into PLA or g-PLA, due to the transition of metastable α′ form crystal to the stable α form crystal of PLA.[30] Similar results were also observed with gradual increase of microfibrillated cellulose (MFC) loading in a study by Song *et al.*[31] In that specific work, it was observed that the small exothermic peaks disappeared on the second heating scan curves. In the cooling scans shown in Fig. 2c, exothermic peaks with low intensity were observed for the pure PLA and g-PLA samples, indicating a rather low crystallization capability. In the case of PLA samples filled with 1% wt of CNC, the crystallization peaks had relatively higher intensity and started from higher temperature as a result of enhanced tendency to crystallize. The nucleation effect was remarkably enhanced when homogeneous cellulose nanocrystal dispersion in PLA and their good interaction with the matrix are achieved.[32] In the second heating process (Fig. 2d and Table 4), we observed that the T_g, T_{cc} and T_m showed the same tendency as in the first heating scan. Specifically, it has to be observed that, even at the second heating, the combination of g-PLA with CNC favoured the nucleation effect and the crystal growth, with higher crystallinity values obtained for g-PLA/PLA-1CNC (24.4%), g-PLA-1CNC/PLA (24.1%) and g-PLA/PLA/1CNC (23.2%). DSC test results clearly evidenced that the use of a masterbatch approach, *i.e.* the premixing the CNC fillers with PLA or g-PLA, can be considered as an effective method to improve the CNC homogeneous dispersion and crystallization ability of resulted PLA nanocomposites.

Thermogravimetric analysis

TG and DTG curves of neat PLA and PLA based nanocomposites are shown in Fig. 3a and b, respectively. Thermal parameters including T_{onset}, T_{max} and residual mass calculated at 600 °C were summarize in Table 5. T_{onset} of neat PLA was 259.0 °C, while were 262.6 and 269.2 °C for PLA/1CNC and g-PLA/PLA-1CNC, respectively. Similar tendency was also observed in the case of g-PLA, g-PLA/1CNC and g-PLA/PLA-1CNC films,

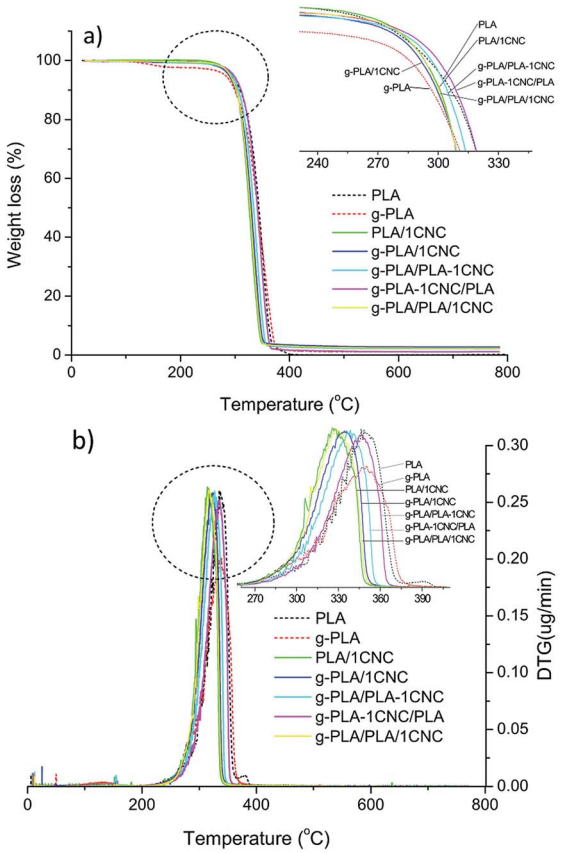

Fig. 3 TG (a) and DTG (b) curves of neat PLA, g-PLA and PLA nanocomposite systems obtained by different masterbatch procedures.

Table 5 Thermal parameters derived from TGA ($T_{onset(1\%)}$, T_{max} and residual mass (%) at 600 °C) for PLA and PLA nanocomposites

Materials	$T_{onset(1\%)}$ (°C)	T_{max} (°C)	Residual mass (%) @ 600 °C
PLA	259.0	351.1	0.04
g-PLA	263.4	352.8	1.05
PLA/1CNC	262.6	328.2	2.37
g-PLA/1CNC	263.4	337.0	2.75
g-PLA/PLA-1CNC	269.2	341.1	2.21
g-PLA-1CNC/PLA	265.9	348.9	1.11
g-PLA/PLA/1CNC	268.7	330.8	2.39

indicating that both CNC and GMA improved the heat resistance of resulted nanocomposites. For g-PLA/PLA-1CNC, g-PLA-1CNC/PLA, and g-PLA/PLA/1CNC, T_{onset} kept the same level, however T_{max} of g-PLA/PLA-1CNC (341.1 °C) and g-PLA-1CNC/PLA (348.9 °C) showed a remarkable improvement with respect of g-PLA/PLA/1CNC (330.8 °C), demonstrating that the preparation of masterbatches *via* pre-incorporation of 1% wt of CNC into PLA or g-PLA was a favourable method to enhance the thermal stability of CNC reinforced PLA nanocomposites. The increased T_{max} for g-PLA/PLA-1CNC and g-PLA-1CNC/PLA, compared with PLA/1CNC and g-PLA/1CNC, respectively, may be attributed to the increased crystallinity due to the more homogeneous dispersion of CNC (discussed in DSC section), and this result was in agreement with the study by Shi *et al.*[33] The reduction of T_{max} for 1% wt of CNC containing PLA nanocomposites, compared with neat PLA and g-PLA, was also observed in some other studies.[34–36]

Moreover, the addition of CNC increased the char yield (residual mass): increased char formation can limit the production of combustible gases, decreasing the exothermicity of the pyrolysis reaction, and inhibiting the thermal conductivity of the burning materials.[37,38]

Tensile properties

Fig. 4a–c show the tensile test results and the typical stress–strain curves (Fig. 4d) for all studied materials. The neat polymeric matrices (neat PLA and g-PLA) exhibited a step-by-step failure process, while the nanocomposites showed a brittle failure process, as a result of the incorporation of rigid CNC particles. In premixing of CNC with PLA system, the addition of 1% wt of CNC (PLA/1CNC) resulted in σ reaching 52.8 MPa, a 19% increase over the neat PLA (44.3 MPa). Furthermore, higher σ (54.2 MPa) and E (2319.0 MPa) were obtained in the case of g-PLA/PLA-1CNC, with an increase of 22.3% and 18.6% compared to PLA, respectively, due to the presence of g-PLA and better dispersion of CNC nanofillers. The same tendency could also be seen in the case of g-PLA, g-PLA/1CNC and g-PLA-1CNC/PLA, being σ and E of the two CNC containing systems increase of 26.2% and 23.7% compared with g-PLA, respectively. Obviously, the effect of changes on ε_b was just the opposite of that on σ and E, and it can be attributed to the presence of rigid nanocrystals, as confirmed in many previous studies.[6,18,32,39] The important improvements observed in the CNC-filled PLA systems may be ascribed to the uniform distribution of CNC in the PLA matrix, and to the strong interfacial adhesion between

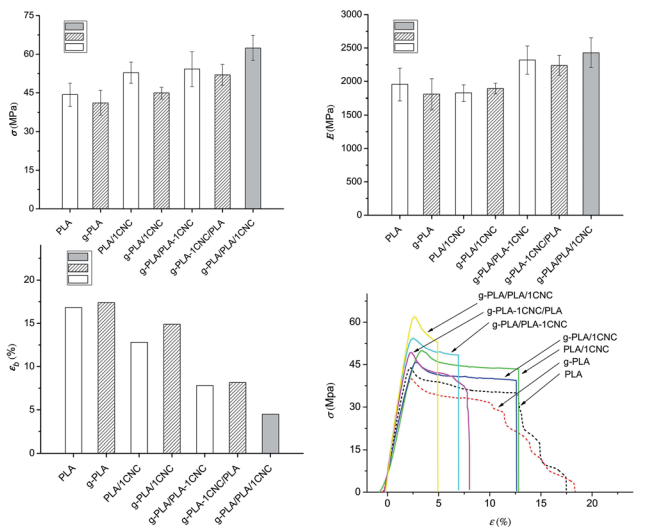

Fig. 4 Values for tensile strength (a), Young's modulus (b), elongation at break (c) and stress–strain curves for neat PLA, g-PLA and PLA nanocomposite systems (d) obtained by different masterbatch procedures.

CNC and PLA matrix. It was believed that the presence of g-PLA would inhibit self-aggregation promoting the CNC dispersion.

In the g-PLA/PLA/1CNC system, maximum values of tensile strength (σ) (62.4 MPa) and elastic modulus (E) (2428.2 MPa), with a minimum of elongation at break (ε_b) (5.0%) were observed, confirming the creation of a rigid network formed among the cellulose nanocrystals in the nanocomposites, which greatly facilitated the enhancement of strength and modulus; at the same time, the appearance of the rigid network and self-aggregation may have slightly damaged the original PLA polymer structure, resulting in a decreased elongation of the composite.[8] The tensile results were in agreement with the DSC tests, confirming how the use of masterbatches could effectively improve the mechanical performance of resulted CNC reinforced PLA nanocomposites. The different mechanical performance detected from g-PLA/PLA-1CNC, g-PLA-1CNC/PLA and g-PLA/PLA/1CNC were considered to contribute to extend applications of PLA based composites as food packaging materials in different sectors.

Morphological analysis

FESEM micrographs of CNC and fractured surfaces of the neat PLA and its nanocomposites are presented in Fig. 5. CNC aggregates (individualized with typical dimensions ranging from 100 to 200 nm in length and 5–10 nm in width) were not visible in all the fractured surfaces, indicating a good dispersion and homogeneous distribution of CNC in the nanocomposites.

While a smooth fracture surface could be seen in neat PLA, an irregular surface was observed in the PLA/1CNC system. Interestingly, the g-PLA/PLA-1CNC film showed a more flat surface compared to PLA/1CNC due to the presence of g-PLA. The fracture surface of PLA and g-PLA samples exhibited a distinct difference because of a plasticizing effect due to the presence of GMA. However, with the loading of 1% wt of CNC, a uniform surface was observed in the case of g-PLA/1CNC, suggesting a good interface adhesion between g-PLA and CNC particles. Compared to pure PLA and g-PLA, the surface of the g-PLA/PLA-1CNC and g-PLA-1CNC/PLA nanocomposites showed no significant differences, as the observed surface regularity of them was between g-PLA and g-PLA/1CNC. The PLA/PLA/1CNC system, with respect of g-PLA/PLA-1CNC and g-PLA-1CNC/PLA, had a rougher fracture surface, since some sawtooth-shape traces and cracks could be observed, which evidenced the more brittle tendency of this system to break. The observed morphological results were consistent with tensile tests (Fig. 4), confirming that the use of a masterbatch approach would be beneficial to the dispersion of cellulose nanostructures in the nanocomposites.

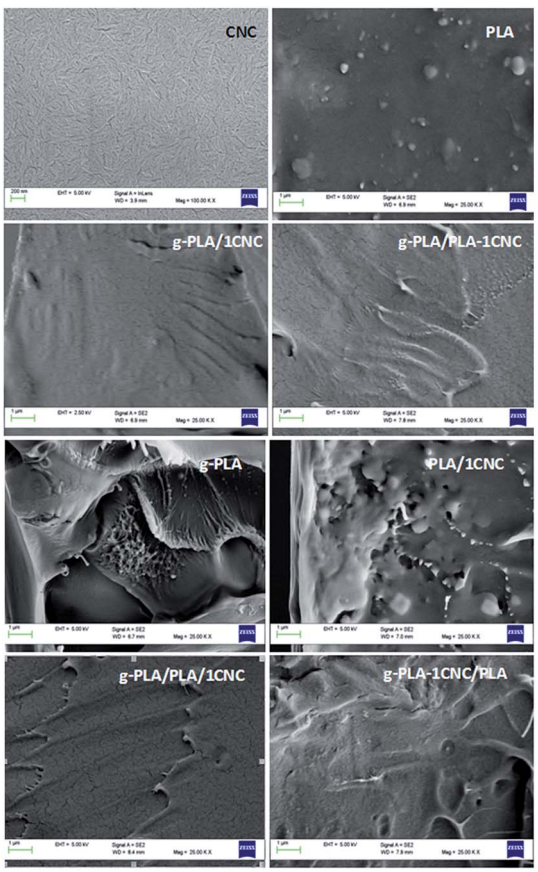

Fig. 5 FESEM images of cellulose nanocrystals (CNC) and fractured samples of neat PLA, g-PLA and PLA nanocomposite systems obtained by different masterbatch procedures.

Conclusions

Poly(lactic acid)/cellulose nanocrystal based nanocomposites were produced by means of different masterbatch approaches, *i.e.* materials were prepared by extrusion of premixed 1% wt CNC in PLA or glycidyl methacrylate grafted PLA (g-PLA), followed by film processing of the different obtained formulations. The morphology studies showed that a relatively good dispersion was achieved, since smoother surfaces were visible in the fractured surfaces of the g-PLA/PLA-1CNC and g-PLA-1CNC/PLA nanocomposites when compared to g-PLA/PLA/1CNC, indicating that the grafting of GMA onto PLA matrix and the use of masterbatches were favourable methods to obtain more homogeneous distribution of CNC in PLA matrix. It was also found that the use of masterbatches was an effective approach to improve the crystallization ability of resulted PLA nanocomposites, with increased crystallinity values observed in DSC tests. The increase of temperature related to the maximum degradation rate (peaks in DTG curves) suggested that the thermal stability could be also improved applying the masterbatches procedure. The evaluation of the mechanical properties of the neat PLA and its nanocomposites showed that the tensile strength and modulus were notably improved due to the presence of g-PLA and better dispersion of CNC fillers, as an increase of 22.3% of tensile strength and 18.6% of modulus for g-PLA/PLA-1CNC was obtained in comparison with neat PLA, while values of 26.2% and 23.7% were achieved in g-PLA-1CNC/PLA composite with respect of g-PLA. Furthermore, the highest tensile strength and modulus values were registered in g-PLA/PLA/1CNC nanocomposites. This study shows that the melt compounding process using the masterbatches, in combination with the grafting of the polymeric matrix, is a very promising

method to reach good processability of cellulose nanocrystal nanocomposites and achievement of improved mechanical and thermal properties for PLA. The results are supposed to contribute to extend the processing methods and applications for CNC based PLA nanocomposites.

Acknowledgements

W. Y. appreciate the funding support of China Scholarship Council (CSC).

Notes and references

1 E. Fortunati, S. Rinaldi, M. Peltzer, N. Bloise, L. Visai, I. Armentano, A. Jiménez, L. Latterini and J. M. Kenny, *Carbohydr. Polym.*, 2014, **101**, 1122–1133.
2 N. Bitinis, R. Verdejo, J. Bras, E. Fortunati, J. M. Kenny, L. Torre and M. A. López-Manchado, *Carbohydr. Polym.*, 2013, **96**, 611–620.
3 M. Darder, P. Aranda and E. Ruiz-Hitzky, *Adv. Mater.*, 2007, **19**, 1309–1319.
4 P. Bordes, E. Pollet and L. Avérous, *Prog. Polym. Sci.*, 2009, **34**, 125–155.
5 V. P. Martino, R. A. Ruseckaite, A. Jiménez and L. Averous, *Macromol. Mater. Eng.*, 2010, **295**, 551–558.
6 N. Bitinis, E. Fortunati, R. Verdejo, J. Bras, J. M. Kenny, L. Torre and M. A. López-Manchado, *Carbohydr. Polym.*, 2013, **96**, 621–627.
7 M. Jonoobi, J. Harun, A. P. Mathew and K. Oksman, *Compos. Sci. Technol.*, 2010, **70**, 1742–1747.
8 N. Lin, J. Huang, P. R. Chang, J. Feng and J. Yu, *Carbohydr. Polym.*, 2011, **83**, 1834–1842.
9 A. Iwatake, M. Nogi and H. Yano, *Compos. Sci. Technol.*, 2008, **68**, 2103–2106.
10 J. R. Capadona, O. Van Den Berg, L. A. Capadona, M. Schroeter, S. J. Rowan, D. J. Tyler and C. Weder, *Nat. Nanotechnol.*, 2007, **2**, 765–769.
11 J. R. Capadona, K. Shanmuganathan, S. Trittschuh, S. Seidel, S. J. Rowan and C. Weder, *Biomacromolecules*, 2009, **10**, 712–716.
12 J.-M. Raquez, Y. Murena, A.-L. Goffin, Y. Habibi, B. Ruelle, F. DeBuyl and P. Dubois, *Compos. Sci. Technol.*, 2012, **72**, 544–549.
13 K. Littunen, U. Hippi, L.-S. Johansson, M. Österberg, T. Tammelin, J. Laine and J. Seppälä, *Carbohydr. Polym.*, 2011, **84**, 1039–1047.
14 Z. Q. Li, X. D. Zhou and C. H. Pei, *Int. J. Polym. Mater.*, 2010, **59**, 725–737.
15 E. Fortunati, D. Puglia, J. M. Kenny, M. Minhaz-Ul Haque and M. Pracella, *Polym. Degrad. Stab.*, 2013, **98**(12), 2742–2751.
16 P. Stenstad, M. Andresen, B. S. Tanem and P. Stenius, *Cellulose*, 2008, **15**, 35–45.
17 M. Martinez-Sanz, M. A. Abdelwahab, A. Lopez-Rubio, J. M. Lagaron, E. Chiellini, T. G. Williams, D. F. Wood, W. J. Orts and S. H. Imam, *Eur. Polym. J.*, 2013, **49**, 2062–2072.
18 M. Pracella, M. M.-U. Haque and D. Puglia, *Polymer*, 2014, **55**, 3720–3728.
19 M. Arrieta, E. Fortunati, F. Dominici, E. Rayón, J. López and J. Kenny, *Carbohydr. Polym.*, 2014, **107**, 16–24.
20 E. D. Cranston and D. G. Gray, *Biomacromolecules*, 2006, **7**, 2522–2530.
21 E. Fortunati, I. Armentano, Q. Zhou, A. Iannoni, E. Saino, L. Visai, L. A. Berglund and J. M. Kenny, *Carbohydr. Polym.*, 2012, **87**, 1596–1605.
22 J. Liu, H. Jiang and L. Chen, *J. Polym. Environ.*, 2012, **20**, 810–816.
23 O. Martin and L. Avérous, *Polymer*, 2001, **42**, 6209–6219.
24 T. Xu, Z. Tang and J. Zhu, *J. Appl. Polym. Sci.*, 2012, **125**, E622–E627.
25 E. Fortunati, I. Armentano, A. Iannoni and J. M. Kenny, *Polym. Degrad. Stab.*, 2010, **95**, 2200–2206.
26 N. Burgos, V. P. Martino and A. Jiménez, *Polym. Degrad. Stab.*, 2013, **98**, 651–658.
27 D. Wu, L. Wu, L. Wu, B. Xu, Y. Zhang and M. Zhang, *J. Polym. Sci., Part B: Polym. Phys.*, 2007, **45**, 1100–1113.
28 E. Fortunati, I. Armentano, Q. Zhou, D. Puglia, A. Terenzi, L. A. Berglund and J. M. Kenny, *Polym. Degrad. Stab.*, 2012, **97**, 2027–2036.
29 T. Dobreva, J. M. Perena, E. Pérez, R. Benavente and M. García, *Polym. Compos.*, 2010, **31**, 974–984.
30 P. Pan, B. Zhu, W. Kai, T. Dong and Y. Inoue, *Macromolecules*, 2008, **41**, 4296–4304.
31 Y. Song, K. Tashiro, D. Xu, J. Liu and Y. Bin, *Polymer*, 2013, **54**, 3417–3425.
32 A. Pei, Q. Zhou and L. A. Berglund, *Compos. Sci. Technol.*, 2010, **70**, 815–821.
33 Q. Shi, C. Zhou, Y. Yue, W. Guo, Y. Wu and Q. Wu, *Carbohydr. Polym.*, 2012, **90**, 301–308.
34 E. Fortunati, M. Peltzer, I. Armentano, L. Torre, A. Jiménez and J. M. Kenny, *Carbohydr. Polym.*, 2012, **90**, 948–956.
35 M. Kowalczyk, E. Piorkowska, P. Kulpinski and M. Pracella, *Composites, Part A*, 2011, **42**, 1509–1514.
36 E. Fortunati, F. Luzi, D. Puglia, F. Dominici, C. Santulli, J. Kenny and L. Torre, *Eur. Polym. J.*, 2014, **56**, 77–91.
37 D. Van Krevelen, *Polymer*, 1975, **16**, 615–620.
38 R. Liepins and E. Pearce, *Environ. Health Perspect.*, 1976, **17**, 55.
39 M. Bulota, A.-H. Vesterinen, M. Hughes and J. Seppälä, *Polym. Compos.*, 2013, **34**, 173–179.